

BaAl_{1.4}Si_{0.6}O_{3.4}N_{0.6}:Eu²⁺ green phosphors' application for improving luminous performance

My Hanh Nguyen Thi¹, Nguyen Le Thai², Thuc Minh Bui³, Tam Nguyen Kieu⁴

¹Faculty of Mechanical Engineering, Industrial University of Ho Chi Minh City, Ho Chi Minh City, Vietnam

²Faculty of Engineering and Technology, Nguyen Tat Thanh University, Ho Chi Minh City, Vietnam

³Faculty of Electrical and Electronics Engineering, Nha Trang University, Nha Trang City, Vietnam

⁴Faculty of Electrical and Electronics Engineering, Ton Duc Thang University, Ho Chi Minh City, Vietnam

Article Info

Article history:

Received Jul 12, 2022

Revised Mar 7, 2023

Accepted Mar 9, 2023

Keywords:

BaAl_{1.4}Si_{0.6}O_{3.4}N_{0.6}:Eu²⁺

Color homogeneity

Luminous flux

Monte Carlo theory

White light-emitted diodes

ABSTRACT

The molten salt synthesis (MSS) method was used to effectively prepare green phosphors BaAl_{1.4}Si_{0.6}O_{3.4}N_{0.6}:Eu²⁺ (or BSON:Eu²⁺) via one homogeneous sphere-like morphology utilizing NaNO₃ in the form of the reacting agent. The phosphors produced one wide stimulation spectrum between 250 and 460 nm, as well as a significant green emission has a maximum point at 510 nm owing to the 4f⁶5d¹-4f⁷ (⁸S_{7/2}) shifts for Eu²⁺ ions. With illumination under 365 as well as 450 nm, the ideal discharge strengths for the specimen prepared utilizing melted salt would receive a boost of 17% and 13%, surpassing the specimen prepared utilizing the traditional solid-state reaction (SSR) approach. The abatement of concentration for the ions of Eu²⁺ from BSON:Eu²⁺ is 5 mol%. In addition, the interactivity of dipole-dipole would be the cause of said abatement. Heat abatement would be studied utilizing the formation coordinate method with abatement temperature reaching ~200 °C. Elemental mapping as well as power-dispersing X-ray spectroscopy (EDS) spectra demonstrated that the expected BaAl_{1.4}Si_{0.6}O_{3.4}N_{0.6}:Eu²⁺ materials were formed.

This is an open access article under the [CC BY-SA](https://creativecommons.org/licenses/by-sa/4.0/) license.



Corresponding Author:

Tam Nguyen Kieu

Faculty of Electrical and Electronics Engineering, Ton Duc Thang University

No. 19 Nguyen Huu Tho Street, Tan Phong Ward, District 7, Ho Chi Minh City, Vietnam

Email: nguyenkieu@tdtu.edu.vn

1. INTRODUCTION

Because of their minimal energy consumption, extended lifespan, and absence of reliance on contaminants such as mercury, white light-emitted diodes (WLEDs) have lately been considered important solid-state light sources for the next-generation environmentally friendly lighting sector and display systems [1]–[3]. Most white light-emitted diodes (LEDs) on the market today are made up of InGaN blue chips as well as yellow phosphor Y₃Al₅O₁₂:Ce³⁺ (abbreviated as YAG:Ce³⁺). Nevertheless, this kind of white LED has various drawbacks, including insignificant chroma rendition indicator (CRI), huge correlated chromaticity temperature (CCT), as well as a shortage of a full range of visible light owing to the shortage of green and red colors, making it unsuitable for use as an interior light source [4]–[6]. Other two ways are used to handle these issues: employing a blend containing phosphors in red as well as green rather than a yellow phosphor or using close-ultra violet LED (UV LED) chips alongside phosphors in red, green, as well as blue [7], [8]. As a result, BSON:Eu²⁺ is important in increasing the luminous characteristic and quality of white LEDs. Rare earth activated oxynitride/nitride based phosphors garnered significant interest for having excellent performance, amazing chemical stability, and outstanding heat quenching property [9]–[11]. In the literature, some silicon oxynitride/nitride green phosphors have been found. Strong green colors are emitted

by β -sialon:Eu²⁺ and MSi₂O₂N₂:Eu²⁺ (M=Ca, Sr, Ba) [12]–[14]. It was shown that incorporating nitrogen into host lattices triggered via Eu²⁺ or Ce³⁺ results in absorptivity as well as discharge under substantially bigger wavelengths, surpassing the oxide hosts. Ferrero *et al.* [15] investigated the impact of nitridation via (SiN)⁺ substitution for (AlO)⁺ in MAl₂O₄ (M=Ca, Sr, Ba), as well as discovered that BaAl₂O₄ was a superior host lattice for (SiN)⁺ inclusion owing to the huge ionic size of Ba²⁺. Despite their benefits, these oxynitride/nitride phosphors generated by the solid-state reaction (SSR) method at high temperatures necessitate extensive soaking times and other crucial conditions [16]. Furthermore, the SSR oxynitride/nitride phosphors exhibit inadequate chemical uniformity and poor particle shape. As a result, finding a novel synthetic approach to address these limitations is critical. Since Arendt initially used the molten salt synthesis (MSS) approach to manufacture BaFe₁₂O₁₉ and SrFe₁₂O₁₉ in 1973, it has been widely used for the synthesis of electronic ceramic powders as well as several inorganic useful substances [17]–[19]. Molten salts play four roles: i) increasing the rate of reaction and decreasing the temperature of the reaction, ii) increasing the degree of uniformity (the distribution of constituent elements in the solid solution), iii) controlling particle size and shape, and iv) controlling the agglomeration state [20]. As a result, as compared to the SSR technique, the MSS technique would be among the easiest as well as cheapest ways that are employed to procure crystalline, chemically pure, one-stage powders under inferior temperatures, mostly with an inferior overall reacting period with minimum leftover contaminants [21]. Several scholars have successfully obtained luminous substances utilizing this approach, including Gd₂MO₆:Eu³⁺ (M=W, Mo), Y₂O₃:Eu³⁺, and Lu₂O₃:Eu³⁺ [22]. Nevertheless, to the greatest of our understanding, no publication on molten salt synthesis of oxynitride/nitride-based phosphors exists.

In this study, we synthesize BSON:Eu²⁺ oxynitride phosphors using the MSS approach in this study. The effect of molten salt on the shape and luminous characteristics of green phosphors BSON:Eu²⁺ is examined. This phosphor's heat and concentration quenching mechanisms are further described. The phosphor application in WLED two-layered remote phosphor model is also presented. Its influences on chromaticity and luminosity of the generated white light is investigated and discussed to demonstrate the prospect in utilizing BSON:Eu²⁺ for high-power and modern WLED devices.

2. EXPERIMENTAL

2.1. Phosphor synthesizing

The following materials were utilized in the manufacture of BSON:Eu²⁺ oxynitride phosphors: BaCO₃ (A.R.), Eu₂O₃ (99.99%), Al₂O₃ (A.R.), Si₃N₄ (99.9%), and NaNO₃ (A.R.). All raw ingredients were used immediately without being purified. BaCO₃, Eu₂O₃, and Al₂O₃ powders were completely ground and calcined at 1450 °C within 3 hours under a standard MSS procedure. Posterior to chilling to ambient heat level, appropriate amounts of α -Si₃N₄ and molten salt (NaNO₃) were added to the powder, with the mass ratios of raw materials and NaNO₃ being 1:0.5, 1:1, 1:1.5, 1:2, and 1:2.5, and the mixes were heated at 1,300 °C for 6 hours under a N₂/H₂ (8:1) reductive atmosphere. We cooled the powders till they reach room temperature in a furnace, then thoroughly washed with deionized water multiple times to remove the reactant residues and molten salt, then dried using a drying oven under 80 °C for 5 hours. The SSR approach was used to generate samples with the same compositions for comparison of luminescence characteristics and morphology [23].

2.2. Characterizing methods

The scanning electron microscope (SEM) method was used to examine the microstructures of the as-prepared specimens. The products synthesized without utilizing NaNO₃ exhibit a poor crystal shape, an uneven size distribution, and many microscopic particles covering large particles. In contrast, the specimens generated in NaNO₃ medium may be considered monodispersed and nonaggregate. At the same time, the particle size follows a regular distribution. This would be caused by the fluid stage in ionic salt creating an absorption layer on the crystalline phase's surface, as well as throughout the melted salt's reacting activity, the ions of Na⁺ enter the created crystals, preventing assemblage. It should be observed that with the addition of NaNO₃, the morphology of the as-prepared phosphors changes from amorphous particles to regular shapes, with a propensity to become sphere-like. The production of product particles is commonly recognized in the standard MSS technique to be divided into two procedures, comprising the nucleation and the growth, respectively [24].

2.3. Computational approach

For the task of generating illumination having decent performance as well as reasonable discharge hue characteristics, merging certain effective phosphors would be necessary. A second key requirement in the utility of phosphors is their excitability, or if their excitation spectra would be consistent with the pumping LED's discharge. Because of this, phosphors for fluorescent lights, even when thoroughly tuned, are often ineffective for use inside LED devices. Said phosphors would be primarily subjected to excitation via

mercury's discharge bar at 254 nm. Furthermore, particle shape contributes to the variation in strength. According to the matching SEM pictures, the specimen created by the SSR process has poor crystalline, a broad particle-size distribution, and substantial numbers of microscopic fragments covering large particles, resulting in some flaws in the particles that scatter or trap the released illumination [25]–[27].

$$R_C \approx 2 \left[\frac{3V}{4\pi x_c Z} \right]^{1/3} \quad (1)$$

x_c indicates the critical concentration of Eu^{2+} within the host, Z indicates the cation amount for the unit cell that were substituted by Eu^{2+} ion, and V indicates the unit cell's volume. For the expression herein, $V=831.19 \text{ \AA}$, $Z=8$, and $x_c=0.05$ is the ideal doping concentration. As a result, the R_C value is judged to be 15.84 \AA . The nonradiative energy transfer process between Eu^{2+} ions is usually mediated by the exchange interaction or multipolar interaction. Exchange contact, which happens with a substantial overlap between the stimulation and emission spectrums, is commonly utilized to define prohibited transitions. Furthermore, the critical distance for energy transfer is less than 4 \AA . The $4f \rightarrow 5d$ transition of Eu^{2+} ions, on the other hand, is permitted by transition rules, and the critical distance of the as-prepared specimen is substantially greater than 4 \AA . It is shown that exchange contact is not the primary energy transfer mechanism in this kind of phosphor. As a result, the power shift among the ions of Eu^{2+} is primarily accomplished by electrical multipolar contact.

3. RESULTS AND DISCUSSION

Figure 1 displays a reverse shift for BSON: Eu^{2+} dosage as well as yellow YAG: Ce^{3+} . The changes were recorded at three CCTs, including 3,000 K, 4,000 K, and 5,000 K, as presented in Figures 1(a) to 1(c), respectively. Specifically, when the concentration of BSON: Eu^{2+} phosphor surges (5% to 10% wt.), the YAG: Ce^{3+} dosage declines, regardless of CCTs. This reduction in yellow phosphor weight percentage is essential to retain the average values of CCT. Moreover, it is reported that the change in amount of integrating phosphors can influence the absorptivity and dispersion of emitted and light within the WLED device. Thus, using BSON: Eu^{2+} as the second phosphor film for the two-layered remote phosphor module can help modify the scattering and transmission of light to regulate the chroma outcome along with luminous flux within WLEDs. For this reason, the BSON: Eu^{2+} concentration chosen determines the color quality of WLEDs.

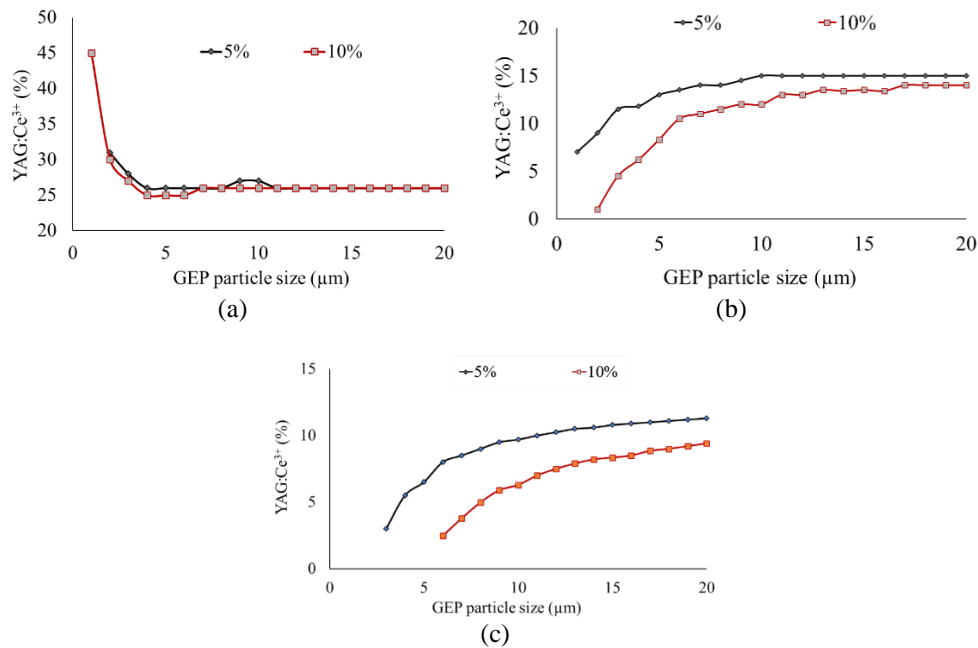


Figure 1. The reduction in YAG: Ce^{3+} concentration as a function of 5 to 10% BSON: Eu^{2+} phosphor content at CCTs of (a) 3,000 K, (b) 4,000 K, and (c) 5,000 K

Figure 2 depicts the photoluminescence spectra in BSON:Eu²⁺ observed under 3,000 K, 4,000 K, as well as 5,000 K in Figures 2(a) to 2(c). The specimens had a wide stimulation band ranging from UV to blue, while the emission spectra had one wide bar (460 to 600 nm) having an intense green emitting peak under 510 nm, which was assigned to the 4f65d1→4f7 shift in divalent europium. The emission spectra were examined underneath the 295 nm stimulation to further confirm that Eu³⁺ is not present. Furthermore, the forms and positions of the stimulation and emission spectra with varying molten salt content are nearly identical. Nevertheless, the luminous strengths of the phosphors made without and with NaNO₃ differ to some amount. The luminescence intensities steadily grow and eventually fall as the molten salt content increases. This is due to the fact that excessive and insufficient liquid phase environments are formed at high and low molten salt content, respectively, resulting in an incomplete reaction that may generate impurity phase. As a result, it suggests that the MSS approach has an ideal molten salt content. As the molten salt content increases, the emission intensities increase because the optimal value is progressively approached, and subsequently fall because the molten salt is too far away from the value. When the mass ratio of raw ingredients and NaNO₃ is 1:2, the specimen exhibits maximum intensities that are 17% and 13% greater than those produced without NaNO₃, under stimulation at 365 and 450 nm, respectively. The reason for this behavior could be that the pure phase is simpler to obtain using NaNO₃ than the specimen acquired utilizing the SSR approach.

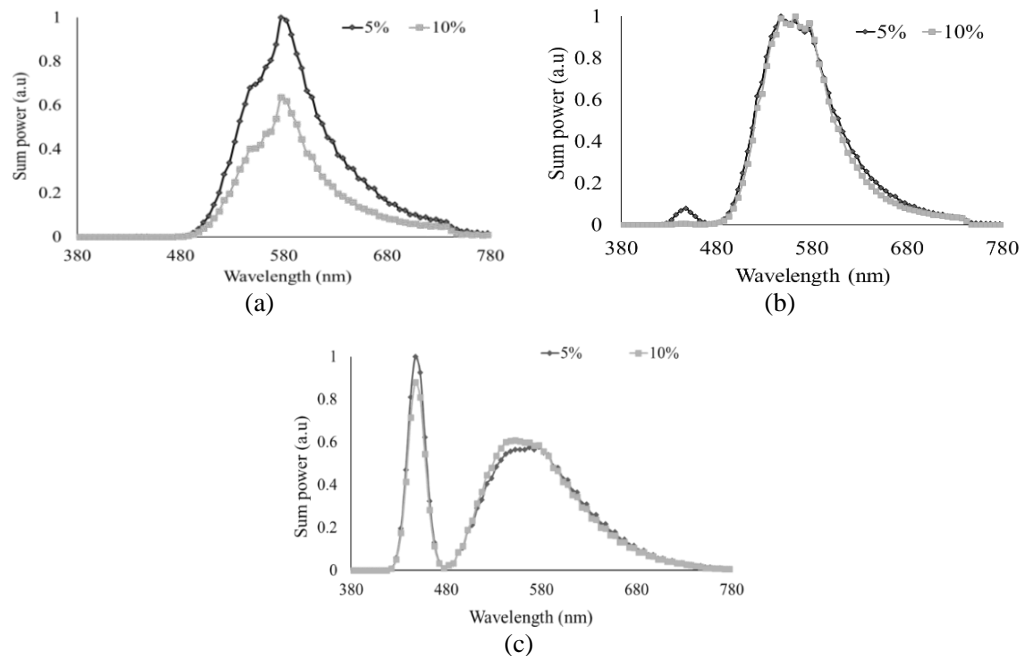


Figure 2. WLED's emission spectra along with BSON:Eu²⁺ concentration: (a) 3,000 K, (b) 4,000 K, and (c) 5,000 K

Figure 3 illustrates the influence of BSON:Eu²⁺ concentration upon the emitted light flux of this dual-sheet remote phosphor layout in the WLED device observed under 3,000 K in Figure 3(a), 4,000 K in Figure 3(b), and 5,000 K in Figure 3(c). The luminous flux emitted surges noticeably when the BSON:Eu²⁺ content is boosted from 5% to 10% by weight. This increase could be attributed to the stronger intensity of wide spectral region of BSON:Eu²⁺ photoluminescence illustrated in Figure 2. The discharge spectra for BSON:Eu²⁺ covers the two emission bands (460 to 480 nm, 500 to 600 nm) which are essential to generate white illumination. The increase for the emission spectra indicates that the illuminating beam is augmented. Furthermore, the WLED's dispersion of blue illumination would be encouraged, implying that the phosphor film's, along with the WLED's dispersion surged, favoring hue consistency.

The hue divergence was considerably reduced alongside said content under every median value of CCT, demonstrated via Figure 4 which contains the data observed under 3,000 K in Figure 4(a), 4,000 K in Figure 4(b) and 5,000 K in Figure 4(c). This phenomenon is the result of the absorption from the green phosphor spheres. When BSON:Eu²⁺ phosphor takes in the blue illumination of the LED chip, BSON:Eu²⁺ granules transmute the illumination into green illumination. Though the yellow light is also absorbed by

BSON:Eu²⁺ particles but it is insignificant when compared to the blue-light one, due to the absorbing qualities offered by the material. As a result of the addition of BSON:Eu²⁺, the amount for green ray for the WLED devices surges, augmenting the hue consistency index. Managing chroma consistency in the remote sheet setting subject to significant heat level, particularly, may become problematic, but BSON:Eu²⁺ can be a potential solution. Besides, hue uniformity is essential for a high-quality WLED lamp. Therefore, if the hue consistency is enhanced, it would increase the price of WLED light. The advantage of employing BSON:Eu²⁺ is its inexpensive cost, making it possible to be commonly applied.

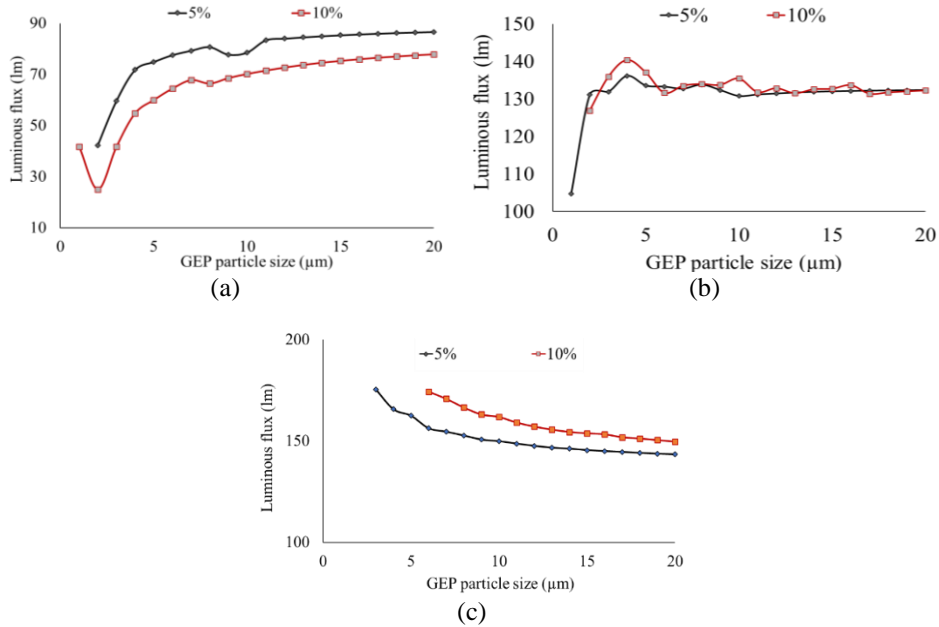


Figure 3. WLED’s lumen along with BSON:Eu²⁺ dosage: (a) 3,000 K, (b) 4,000 K, and (c) 5,000 K

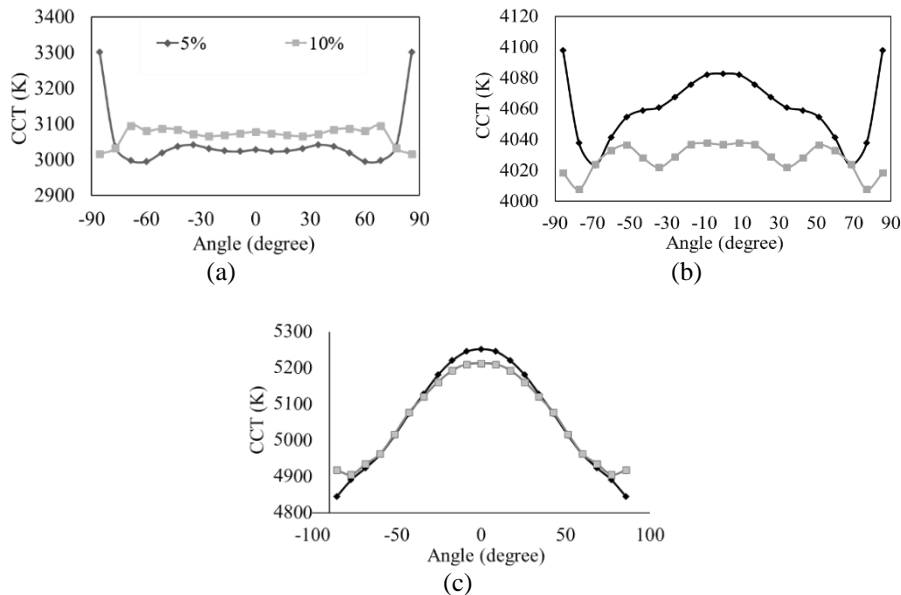


Figure 4. WLED’s CCT along with BSON:Eu²⁺ dosage: (a) 3,000 K, (b) 4,000 K, and (c) 5,000 K

To have good color quality of white light, not only the color coordination but also the color rendition is crucial. Hence, subsequent works provide CRI along with composite quality score (CQS) to

analyze the color rendering and reproducing ability of white-light sources. When CRI is subject to illumination, it assesses authentic chromas in entities. Figure 5 shows a decrease in CRI with the increasing concentration of BSON:Eu²⁺ phosphor under 3,000 K in Figure 5(a), 4,000 K in Figure 5(b), and 5,000 K in Figure 5(c). Regardless, such decreases in CRI would be acceptable since it is merely one limitation of CQS. Particularly, CQS would be more sufficient and efficient for gauging chroma outcomes in WLED, surpassing CRI, because it covers CRI, and hue coordinate, along with beholder's choice. Figure 6 displays the CQS data of WLEDs observing under CCTs of 3,000 K, 4,000 K, and 5,000 K shown via Figures 6(a) to 6(c). The CQS increases alongside the presence of BSON:Eu²⁺ phosphor. Additionally, when the BSON:Eu²⁺ concentration is raised, CQS does not alter considerably with BSON:Eu²⁺ concentrations just under 10% wt. When the BSON:Eu²⁺ content exceeds 10% wt., CRI, as well as CQS, would noticeably shrink, resulting from substantial chroma penalty under green dominance. In particular, the chroma imbalance would be generated through immoderate green light that probably overshadows the blue and yellow ones, consequently decreasing WLED color fidelity. Hence, prior to taking advantage of BSON:Eu²⁺, determining the necessary dosage would be very important.

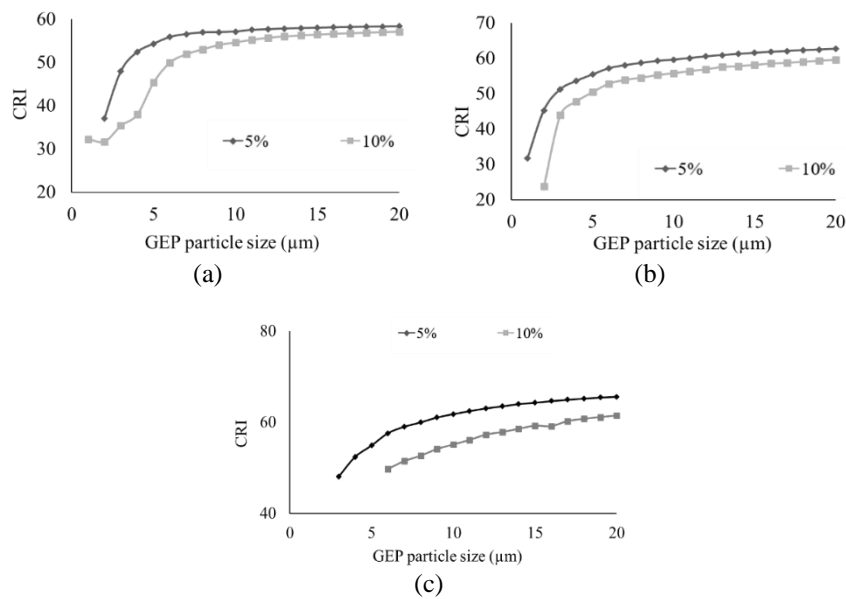


Figure 5. WLED's CRI along with BSON:Eu²⁺ dosage (a) 3,000 K, (b) 4,000 K, and (c) 5,000 K

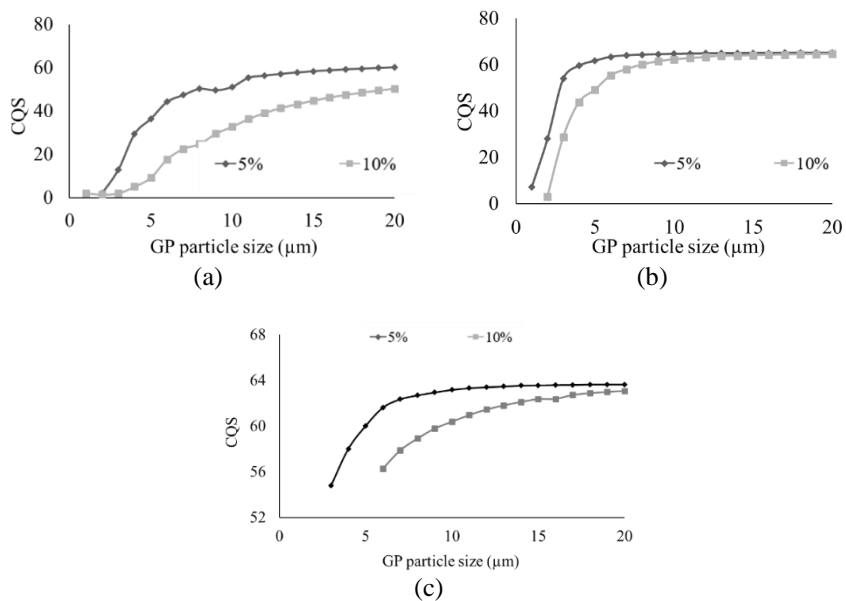


Figure 6. WLED's CQS along with BSON:Eu²⁺ dosage (a) 3,000 K, (b) 4,000 K, and (c) 5,000 K

4. CONCLUSION

Finally, green phosphors $\text{BaAl}_{1.4}\text{Si}_{0.6}\text{O}_{3.4}\text{N}_{0.6}:\text{Eu}^{2+}$ were effectively synthesized utilizing the MSS approach and the reaction medium NaNO_3 . When compared to the SSR-prepared specimen, the emission strengths are raised by 17% and 13%, respectively, under 365 and 450 nm illumination. Because of the usage of molten salt, particles with a homogeneous sphere-like shape, higher crystallization, and improved dispersibility are generated. Because of the energy transfer between Eu^{2+} ions, concentration quenching occurs when the activator doping content is up to 5 mol%. The essential energy transfer distance is calculated to be 15.84 Å, implying that dipole-dipole interactivity would be the key cause of dosage abatement. Furthermore, the T50 thermal quenching temperature may be calculated to be around 200 °C, indicating that this phosphor has a low thermal quenching characteristic. Given the abundance of molten salts, we have reason to assume that an extremely effective molten salt system for a given phosphor can be developed. This suggests that there is still room to improve the shape and luminescence strength of other oxynitride phosphors while also providing an economical and realistic way to address the drawbacks of traditional SSR methods.

REFERENCES

- [1] A. Ullah *et al.*, "Household light source for potent photo-dynamic antimicrobial effect and wound healing in an infective animal model," *Biomedical Optics Express*, vol. 9, no. 3, pp. 1006–1019, Mar. 2018, doi: 10.1364/BOE.9.001006.
- [2] A. Keller, P. Bialecki, T. J. Wilhelm, and M. K. Vetter, "Diffuse reflectance spectroscopy of human liver tumor specimens-towards a tissue differentiating optical biopsy needle using light emitting diodes," *Biomedical Optics Express*, vol. 9, no. 3, pp. 1069–1081, Mar. 2018, doi: 10.1364/BOE.9.001069.
- [3] Y. Peng *et al.*, "Flexible fabrication of a patterned red phosphor layer on a YAG:Ce³⁺ phosphor-in-glass for high-power WLEDs," *Optical Materials Express*, vol. 8, no. 3, pp. 605–614, Mar. 2018, doi: 10.1364/OME.8.000605.
- [4] L. Duan and Z. Lei, "Wide color gamut display with white and emerald backlighting," *Applied Optics*, vol. 57, no. 6, pp. 1338–1344, Feb. 2018, doi: 10.1364/AO.57.001338.
- [5] H.-P. Huang, M. Wei, and L.-C. Ou, "White appearance of a tablet display under different ambient lighting conditions," *Optics Express*, vol. 26, no. 4, pp. 5018–5030, Feb. 2018, doi: 10.1364/OE.26.005018.
- [6] Z. Li, Y. Tang, J. Li, X. Ding, C. Yan, and B. Yu, "Effect of flip-chip height on the optical performance of conformal white-light-emitting diodes," *Optics Letters*, vol. 43, no. 5, pp. 1015–1018, Mar. 2018, doi: 10.1364/OL.43.001015.
- [7] A. I. Alhassan *et al.*, "Development of high performance green c-plane III-nitride light-emitting diodes," *Optics Express*, vol. 26, no. 5, pp. 5591–5601, Mar. 2018, doi: 10.1364/OE.26.005591.
- [8] S. Jost, C. Cauwerts, and P. Avouac, "CIE 2017 color fidelity index Rf: a better index to predict perceived color difference?," *Journal of the Optical Society of America A*, vol. 35, no. 4, pp. 202–213, Apr. 2018, doi: 10.1364/JOSAA.35.00B202.
- [9] X. Ding *et al.*, "Improving the optical performance of multi-chip LEDs by using patterned phosphor configurations," *Optics Express*, vol. 26, no. 6, pp. 283–292, Mar. 2018, doi: 10.1364/oe.26.00a283.
- [10] X. Li, B. Hussain, L. Wang, J. Jiang, and C. P. Yue, "Design of a 2.2-mW 24-Mb/s CMOS VLC receiver SoC with Ambient light rejection and post-equalization for Li-Fi applications," *Journal of Lightwave Technology*, vol. 36, no. 12, pp. 2366–2375, Jun. 2018, doi: 10.1109/JLT.2018.2813302.
- [11] A. Lihachev, I. Lihacova, E. V. Plorina, M. Lange, A. Derjabo, and J. Spigulis, "Differentiation of seborrheic keratosis from basal cell carcinoma, nevi and melanoma by RGB autofluorescence imaging," *Biomedical Optics Express*, vol. 9, no. 4, pp. 1852–1858, Apr. 2018, doi: 10.1364/BOE.9.001852.
- [12] T. Wook Kang *et al.*, "Enhancement of the optical properties of CsPbBr₃ perovskite nanocrystals using three different solvents," *Optics Letters*, vol. 45, no. 18, pp. 4972–4975, Sep. 2020, doi: 10.1364/OL.401058.
- [13] J. Hao, H.-L. Ke, L. Jing, Q. Sun, and R.-T. Sun, "Prediction of lifetime by lumen degradation and color shift for LED lamps, in a non-accelerated reliability test over 20,000 h," *Applied Optics*, vol. 58, no. 7, pp. 1855–1861, Mar. 2019, doi: 10.1364/AO.58.001855.
- [14] Z. Huang, Q. Liu, M. R. Pointer, W. Chen, Y. Liu, and Y. Wang, "Color quality evaluation of Chinese bronzeware in typical museum lighting," *Journal of the Optical Society of America A*, vol. 37, no. 4, pp. 170–180, Apr. 2020, doi: 10.1364/JOSAA.381498.
- [15] A. Ferrero, B. Bernad, J. Campos, N. Richard, C. Fernández-Maloigne, and M. Melgosa, "Goniochromatic assessment of gray scales for color change," *Journal of the Optical Society of America A*, vol. 37, no. 8, pp. 1266–1275, 2020, doi: 10.1364/josaa.394170.
- [16] K. Werfli *et al.*, "Experimental demonstration of high-speed 4×4 imaging multi-CAP MIMO visible light communications," *Journal of Lightwave Technology*, vol. 36, no. 10, pp. 1944–1951, May 2018, doi: 10.1109/JLT.2018.2796503.
- [17] G. Liu, W. Hou, and M. Han, "Unambiguous peak recognition for a silicon Fabry-Pérot interferometric temperature sensor," *Journal of Lightwave Technology*, vol. 36, no. 10, pp. 1970–1978, May 2018, doi: 10.1109/JLT.2018.2797202.
- [18] H.-L. Ke *et al.*, "Lumen degradation analysis of LED lamps based on the subsystem isolation method," *Applied Optics*, vol. 57, no. 4, Feb. 2018, doi: 10.1364/AO.57.000849.
- [19] L. Xiao, C. Zhang, P. Zhong, and G. He, "Spectral optimization of phosphor-coated white LED for road lighting based on the mesopic limited luminous efficacy and IES color fidelity index," *Applied Optics*, vol. 57, no. 4, pp. 931–936, Feb. 2018, doi: 10.1364/AO.57.000931.
- [20] H. Lee, S. Kim, J. Heo, and W. J. Chung, "Phosphor-in-glass with Nd-doped glass for a white LED with a wide color gamut," *Optics Letters*, vol. 43, no. 4, pp. 627–630, Feb. 2018, doi: 10.1364/OL.43.000627.
- [21] H. Daicho, K. Enomoto, H. Sawa, S. Matsuishi, and H. Hosono, "Improved color uniformity in white light-emitting diodes using newly developed phosphors," *Optics Express*, vol. 26, no. 19, Sep. 2018, doi: 10.1364/OE.26.024784.
- [22] J. X. Yang, D. S. Li, G. Li, E. Y. B. Pun, and H. Lin, "Photon quantification in Ho³⁺/Yb³⁺ co-doped opto-thermal sensitive fluorite glass phosphor," *Applied Optics*, vol. 59, no. 19, pp. 5752–5763, Jul. 2020, doi: 10.1364/AO.396393.
- [23] Z. Zhao, H. Zhang, S. Liu, and X. Wang, "Effective freeform TIR lens designed for LEDs with high angular color uniformity," *Applied Optics*, vol. 57, no. 15, pp. 4216–4221, May 2018, doi: 10.1364/AO.57.004216.
- [24] H.-Y. Yu *et al.*, "Solar spectrum matching with white OLED and monochromatic LEDs," *Applied Optics*, vol. 57, no. 10, Apr. 2018, doi: 10.1364/AO.57.002659.

- [25] N. Anous, T. Ramadan, M. Abdallah, K. Qaraqe, and D. Khalil, "Impact of blue filtering on effective modulation bandwidth and wide-angle operation in white LED-based VLC systems," *OSA Continuum*, vol. 1, no. 3, Nov. 2018, doi: 10.1364/OSAC.1.000910.
- [26] T. DeLawyer, M. Tayon, C. Yu, and S. L. Buck, "Contrast-dependent red-green balance shifts depend on S-cone activity," *Journal of the Optical Society of America A*, vol. 35, no. 4, pp. 114–121, Apr. 2018, doi: 10.1364/JOSAA.35.00B114.
- [27] H. Lee *et al.*, "Color-tunable organic light-emitting diodes with vertically stacked blue, green, and red colors for lighting and display applications," *Optics Express*, vol. 26, no. 14, Jul. 2018, doi: 10.1364/OE.26.018351.

BIOGRAPHIES OF AUTHORS



My Hanh Nguyen Thi     received a Bachelor of Physics from An Giang University, Vietnam, Master of Theoretical Physics and Mathematical Physics, Hanoi National University of Education, Vietnam. Currently, she is a lecturer at the Faculty of Mechanical Engineering, Industrial University of Ho Chi Minh City, Vietnam. Her research interests are Theoretical Physics and Mathematical Physics. She can be contacted at: nguyenthimyhanh@iuh.edu.vn.



Nguyen Le Thai     received his BS in Electronic Engineering from Danang University of Science and Technology, Vietnam, in 2003, MS in Electronic Engineering from Posts and Telecommunications Institute of Technology, Ho Chi Minh, Vietnam, in 2011 and PhD degree of Mechatronics Engineering from Kunming University of Science and Technology, China, in 2016. He is currently with the Nguyen Tat Thanh University, Ho Chi Minh City, Vietnam. His research interests include the renewable energy, optimization techniques, robust adaptive control and signal processing. He can be contacted at nlthai@nttu.edu.vn.



Thuc Minh Bui     got his B.S. and M.S. degrees in Electrical Engineering from Ho Chi Minh City University of Technology and Education in 2005 and 2008, respectively, and his Ph.D. degree in electrical engineering at from Yeungnam University in Gyeongsan, Korea, in 2018. He is currently a lecturer at the Faculty of Electrical and Electronics Engineering at Nha Trang University in Nha Trang City, Vietnam. His scientific interests include control theory, power converter, automation, and optical science with applications to industry and the environment. He can be reached via minhbt@ntu.edu.vn.



Tam Nguyen Kieu     was born in Phu Yen Province, Vietnam. He received his M.Sc. from university of transport and communications, Viet Nam in 2012 and defended his PhD. diploma at VSB-Technical University of Ostrava, Czech Republic. His research interests include the wireless communication, WiMax, energy harvesting, and optics. He can be contacted at nguyenkietam@tdtu.edu.vn.